HHS Public Access

Author manuscript

J Immunol. Author manuscript; available in PMC 2019 October 15.

Published in final edited form as:

J Immunol. 2018 October 15; 201(8): 2452–2461. doi:10.4049/jimmunol.1800537.

LFA-1 Ligation by High Density ICAM-1 is Sufficient to Activate IFN-γ Release by Innate T lymphocytes

Akshat Sharma[*], **Stephanie M. Lawry**[*], **Bruce S. Klein**[*], **Xiaohua Wang**[†], **Nathan M. Sherer**[††], **Nicholas A. Zumwalde**[*], and **Jenny E. Gumperz**[*]

[*] Department of Medical Microbiology and Immunology, University of Wisconsin School of Medicine and Public Health, Madison, WI 53706, USA

[†] Address TBD

[††] Department of Oncology, University of Wisconsin School of Medicine and Public Health, Madison, WI 53706, USA

Abstract

By binding to its ligand ICAM-1, LFA-1 is known to mediate both adhesion and co-stimulatory signaling for T cell activation. The constitutively high LFA-1 cell surface expression of invariant natural killer T (iNKT) cells has been shown to be responsible for their distinctive tissue homing and residency within ICAM-rich endothelial vessels. However, the functional impact of LFA-1 on the activation of iNKT cells and other innate T lymphocyte subsets has remained largely unexplored. In particular, it is not clear whether LFA-1 contributes to innate-like pathways of T cell activation, such as IFN-γ secretion in response to IL-12. Using recombinant ICAM-1-Fc to stimulate human iNKT cells in the absence of APCs, we show that LFA-1 engagement enhances their IL-12-driven IFN-γ production. Surprisingly, exposure to high densities of ICAM-1 was also sufficient to activate iNKT cell cytokine secretion independently of IL-12 and associated JAK/STAT signaling. LFA-1 engagement induced elevated cytoplasmic Ca^{++} and rapid ERK phosphorylation in iNKT cells, and the resulting IFN-γ secretion was dependent on both of these pathways. Analysis of freshly isolated human PBMC samples revealed that a fraction of lymphocytes that showed elevated LFA-1 cell surface expression produced IFN-γ in response to plate-bound ICAM-1-Fc. A majority of the responding cells were T cells, with the remainder NK cells. The responding T cells included iNKT cells, MAIT cells, and $V\delta2^{+}$ γδ T cells. These results delineate a novel integrin-mediated pathway of IFN-γ secretion that is a shared feature of innate lymphocytes.

Introduction

T cells are typically considered to epitomize adaptive immunity. However, it has recently become clear that a fraction of T lymphocytes share with innate lymphocytes the expression of a master transcription factor, Promyelocytic Leukemia Zinc Finger (PLZF) (1). PLZF is required for the proper development of innate lymphoid cells (ILCs) and human NK cells, and is expressed in both of these subsets in the periphery (2, 3). Thus, PLZF is associated

Corresponding author: Jenny E. Gumperz, Tel (608) 263-6902, Fax (608) 262-8418, jegumperz@wisc.edu.

with an innate functional status of lymphocytes. The best known PLZF^{+} T cells are invariant natural killer T (iNKT) cells (4–6). iNKT cells utilize a canonical TCRα chain rearrangement that is paired with a limited set of TCRβ chains, recognize conserved lipid antigens presented by non-classical CD1d antigen presenting molecules, and have innate-like functional properties including mediating rapid effector cytokine responses upon primary challenge (7–10). Additional subsets of T lymphocytes now known to express PLZF include mucosal-associated invariant T (MAIT) cells and certain γδ T cells (11, 12). These subsets resemble iNKT cells in that they utilize canonical TCR rearrangements, recognize conserved non-classical antigens, and have innate-like functional properties (13–18). Thus, based on their constrained TCR structures, specificity for conserved ligands, and shared transcriptional program, these T cell subsets can be grouped into a distinct compartment called “innate T lymphocytes” (1, 19, 20). The specific features of innate T cells that are conferred by their shared expression of PLZF, and that may thus set them apart as a group from adaptive T lymphocytes, remain largely unexplored.

One such distinctive characteristic conferred by PLZF is upregulated expression of the integrin Leucocyte Function-associated Antigen-1 (LFA-1) (21). LFA-1 plays critical roles in T cell migration via binding to its adhesion ligand Intracellular Adhesion Molecule-1 (ICAM-1), which is expressed on vascular endothelium and other cell types (22) The elevated LFA-1 expression of murine iNKT cells has been shown to be responsible for their stable residency in the sinusoids of the liver, which are endothelial vessels that are high in ICAM-1 (21, 23). Similarly, under steady state conditions iNKT cells have been observed by intravital microscopy to constitutively patrol other ICAM-rich areas of the vasculature, including pulmonary endothelial surfaces (24). Additionally, both human and murine iNKT cells have been found to be recruited to atherosclerotic plaques, which are inflamed vascular endothelial areas where ICAM-1 levels may be elevated (25–29). Thus, the elevated LFA-1 expression level of iNKT cells likely plays a key role in their distinctive tissue recruitment and residency patterns. However, what has been less clear is whether their high LFA-1 status impacts the functional responses of iNKT cells.

LFA-1 also plays a key role during TCR-mediated activation. TCR signaling from initial antigen recognition induces the unfolding of LFA-1 from its low-affinity state into higher affinity conformations that are able to bind to ICAM-1 (30). LFA-1 binding to ICAM-1 binding leads to the rapid activation of Src-family kinases (e.g. Lck, ZAP-70) and an ensuing signaling cascade resulting in the activation of PLCγ and triggering of downstream Ca^{++} signaling (31–33). Ultimately, the signaling events contributed by LFA-1 are thought to lower the threshold of antigen required for productive T cell activation (34, 35). iNKT cells are known to recognize certain unusual glycolipids, such as α-galactosylceramide (α-GalCer), as highly potent TCR agonists (9, 36, 37). However, it is not clear that many pathogenic microbes produce α-GalCer or closely related lipids, and lipids of this type derived from other physiological sources appear to be present in only extremely small quantities (38, 39). In contrast, other highly abundant lipid species (e.g. lyso-phosphatidylcholine and β-linked glycosylsphingolipids) serve as weak TCR agonists for iNKT cells (40–43). Thus, since iNKT cells probably experience only low levels of TCR stimulation in most physiological settings due to a scarcity of high affinity and/or an

abundance of low affinity antigens, LFA-1 mediated co-stimulation likely plays an important role during their TCR-mediated activation.

Less clear is whether LFA-1 also impacts other pathways of iNKT cell activation. For example, iNKT cells can also become activated directly by pro-inflammatory cytokines (e.g. IL-12), without requiring a concurrent TCR signal (44–47). Indeed, prior studies in murine models of bacterial infection have suggested that TCR signaling is not required (48), and instead the cytokine-dependent pathway of activation is a dominant means by which iNKT cells become activated during many bacterial infections *in vivo* (49–51). It has been established that the IFN-γ produced by adaptive T cells in response to TCR stimulation is secreted in a directional manner towards the immunological synapse, which is also where LFA-1 is aggregated at the cell surface (52), and we have observed a similar phenomenon for iNKT cells responding to DCs presenting the potent lipid antigen α-GalCer (supplementary Figure 1A). However, in the case of TCR-independent IFN-γ secretion by iNKT cells, it is not clear whether cell contact, and thus LFA-1 engagement, plays any role. This is an important question, since the physiological effects of IFN-γ secretion probably depend largely on the identity and functional characteristics of the recipient cells, and thus IFN-γ that is produced in the context of an immunological synapse with an APC may serve a different purpose than IFN-γ that is produced during contact with other cells, or that is produced in a manner that is independent of cell contact.

We previously observed that cytokine-stimulated human iNKT cells secreted substantially more IFN-γ when B-lymphoblastoid cells were also present, even if the B-lymphoblastoid cells lacked CD1d and thus were not able to deliver TCR stimulation to the iNKT cells (47). Moreover, the IFN-γ produced by iNKT cells during exposure to IL-12 on an ICAM-1 coated surface appeared to co-localize intracellularly with the tubulin nexus representing the microtubule organizing center (supplementary Figure 1B), which has been shown in migrating T cells to be positioned adjacent to the area of the plasma membrane where LFA-1 is aggregated (53). Finally, it has also been observed through intravital microscopic analysis that intravenous injection of the cytokines IL-12 and IL-18 leads to rapid IFN-γ production by the iNKT cells patrolling hepatic sinusoids (54). Intriguingly, the iNKT cell response in this situation was associated with migration arrest, suggesting that it was associated with conformational changes and signaling by LFA-1. Together, these observations suggested to us that LFA-ICAM interactions might facilitate or enhance TCR-independent IFN-γ secretion by iNKT cells. Therefore, in this analysis we set out to investigate the impact of LFA-1 engagement on TCR-independent IFN-γ secretion by iNKT cells.

Materials and Methods

Peripheral blood mononuclear cell (PBMC) isolation.

Venous blood was obtained from healthy adult male or female subjects in accordance with a UW-IRB approved protocol. Freshly drawn blood samples were mixed with heparin sodium (10U per ml of blood) (Sagent Pharmaceuticals), and mononuclear cells were purified by density-gradient centrifugation (Ficoll-Paque Premium; GE Healthcare).

iNKT cells.

Human iNKT cells used in these analyses included clonal lines that we have previously established (40, 49, 55–57), and polyclonal cultures resulting from short-term in vitro expansion of cells sorted using α-GalCer loaded CD1d tetramer provided by the NIH tetramer facility at Emory University, as we have previously described (58, 59). Clonal and polyclonal iNKT cell cultures were maintained in culture medium comprised of RPMI 1640 diluted with glucose-free RPMI (Biolgical Industries) to yield a final glucose concentration of 7.5mM, 3% human AB serum (Atlanta Biologicals), 10% heat-inactivated bovine calf serum (HyClone), 1% Penicillin-Streptomycin, 1% L-glutamine and 200 U/ml IL-2 (Peprotech). iNKT cultures used for experiments were of 98–100% purity as assessed by flow cytometric analysis with α-GalCer loaded CD1d tetramers.

ICAM-1 stimulation of iNKT cells.

High protein-binding 96-well plates (Corning) were coated with recombinant human ICAM-1-Fc (Acro Biosystems) or an isotype-matiched negative control mAb (clone MOPC21, Sigma Aldrich), then washed with PBS to remove unbound ICAM-1. iNKT cells (50×10^5 per well) were added in culture medium lacking IL-2. Where indicated, the following compounds were included in the culture medium: 20 U/ml recombinant human IL-12p70 (Peprotech); the indicated concentrations of U0126 (Invivogen) or Cyclosporin A (Sigma Aldrich); 1 μg/ml anti-human CD11a blocking mAb (Invitrogen, Clone HI111); 1 μg/ml anti-human CD18 blocking mAb (Biolegend, Clone TS1/18); 5 μg/ml anti-CD1d blocking mAb (clone CD1d55); or the indicated concentrations of JAK Inhibitor I (Calbiochem). Where indicated, instead of ICAM-Fc simulation the iNKT cells were exposed to plate-bound CD1d-Fc that had been pulsed with 25 ng/ml α-GalCer, as previously described (40). Each stimulation condition was performed in 3–4 replicate wells. iNKT cells were stimulated for 18–24h at 37 ^{o}C and 5% $C0_2$, then culture supernatants were harvested and assayed for IFN-γ using a sandwich ELISA (capture antibody clone MD-1 from Biolegend; biotinylated detection antibody clone 4SB.3 from BD Pharmingen). IFN-γ concentrations were determined by comparison to a standard curve of recombinant human IFN-γ (Peprotech) assayed in parallel.

Microscopic analysis of iNKT cell cytoplasmic Ca^{++}.

iNKT cells were labeled with Fluo-4 (Calbiochem) according to the manufacturer's instructions, then 7.5×10^4 cells were seeded onto glass chamber slides (iBidi) coated with a 1 μg/ml or a 5 μg/ml solution of ICAM-1-Fc and blocked with 2.5% BSA, or coated with poly-L-Lysine. The slides were placed into a 37 ^{o}C and 5% CO_2 chamber, and images were taken every 20 seconds for 30 minutes using a Nikon Ti-Eclipse inverted wide-field microscope. For analysis of Fluo-4 signal intensity, 25 iNKT cells from each condition were chosen randomly at a single time-point based on bright field images, and the fluorescence intensity of each cell was determined using FIJI/ImageJ2 software (imagej.net/Fiji). For analysis of Fluo-4 signal over time, live cells were manually tracked over 30 minutes (90 frames) with the changes in 2-D mean fluorescence intensity (MFI) gauged on a per cell basis.

Detection of ERK phosphorylation.

Jurkat T cells (2×10^6) or iNKT cells (1.5×10^6) were stimulated with anti-human CD11a mAb (Biolegend, Clone TS2/4) for the indicated times in culture medium lacking IL-2. Cells were lysed using CellLytic-M™ (Sigma Aldrich) buffer infused with one tablet of Phosphostop™ (Roche) phosphatase inhibitor. Lysates were run on a 12% SDS-PAGE gel, then transferred onto a polyvinylidene difluoride (PVDF) membrane using a Transblot Turbo™ semi-dry transfer system (Biorad). Membranes were blocked overnight at 4 °C in a solution of Tris-buffered saline, 0.05% Tween-20, 5% non-fat dry milk (Sanalac), 5% bovine serum albumin (Fisher). Phosphorylated or total ERK bands were detected using a polyclonal rabbit anti-human phospho-ERK antibody (Cell Signaling Technology; Cat# 9101S) or polyclonal rabbit anti-human MAPK p44/42 ERK1/2 antibody (Cell Signaling Technology, Cat# 9102S), followed by detection using a goat anti-rabbit HRP-linked secondary antibody (Cell Signaling Technology; Cat# 7074S). Membranes were developed with Clarity Western ECL Substrate™ (Biorad) and analyzed using a VersaDoc Imaging System (Biorad). Total and phospho-ERK band intensities were quantitated using FIJI/ImageJ software. For flow cytometric detection of ERK phosphorylation, iNKT cells (1×10^6) were stimulated with anti-human CD11a mAb (clone: TS2/4; Biolegend) for 5 minutes, followed by fixation using Biolegend's Fixation Buffer (Cat# 420801) and permeabilized with chilled True-Phos™ buffer (Biolegend). Cells were then stained with anti-phospho-ERK mAb (clone: 4B11B69; Biolegend) or isotype control mAb for 30 minutes in darkness at room temperature. Samples were read on an LSR II flow cytometer (BD Biosciences), and data were analyzed using FlowJo software (Tree Star Inc).

ICAM-Fc stimulation of fresh PBMCs.

PBMCs (1×10^5) were incubated for 18–24 hrs with plate-bound ICAM-1-Fc (coated at 5 μg/ml) or with an isotype-matched negative control mAb (5 μg/ml MOPC-21, Sigma Aldrich). PBMCs were resuspended and Fc receptors were blocked by incubation in a solution of PBS containing 25% human AB serum (Atlanta Biologicals) for 20 minutes at 4°C, then cell-surface staining was performed for 30 minutes at 4 °C using the following human-specific antibodies or tetramers: anti-CD3 (OKT3, Biolegend), anti-CD4 (OKT4, Biolegend), anti-CD8α (HIT8a, Biolegend), anti-CD8β (SIDI8BEE, eBioscience), anti-CD11a (HI111, Biolegend), anti-CD56 (5.1H11, Biolegend), CD1d tetramer (PBS-57 loaded, NIH Tetramer Core Facility), MR1 tetramer (5-OP-RU loaded, NIH Tetramer Core Facility), anti-Vδ2 TCR (123R3, Miltenyi Biotec). Cells were fixed and permeabilized according to the manufacturer's instructions using the BD Cytofix/Cytoperm kit (BD Biosciences), then stained with anti-IFN-γ (4S.B3, Biolegend), anti-PLZF (Mags.21F7, eBioscience), or the respective negative control mAbs suggested by the vendor. Cells were then washed, resuspended in PBS and analysed on an LSR II flow cytometer (BD Biosciences). Staining data were analyzed using FlowJo analysis software (Tree Star Inc).

Statistical Analyses.

An unpaired two-sided Student's T-test was used to assess replicates from different experimental conditions. A Mann-Whitney test was used to assess sample groups comprised

of data aggregated from multiple independent analyses. Sets of paired samples were analyzed using a Wilcoxon-matched pairs analysis.

Results

ICAM-1binding to LFA-1 co-stimulates cytokine-driven IFN-γ secretion by human iNKT cells

Since it was previously shown in a murine model system that PLZF confers elevated LFA-1 expression, and murine iNKT cells have constitutively high levels of this integrin (21), we first sought to confirm whether human iNKT cells also show high expression of LFA-1. PBMCs purified from healthy adult subjects were stained for CD3 to identify T cells, and co-stained for CD11a to detect LFA-1, and CD1d tetramer to distinguish iNKT cells. Flow cytometric analysis revealed that the iNKT cells were amongst the brightest CD11a-expressing T cells (Figure 1A, left plots). Analysis of samples from multiple unrelated donors revealed that this was consistently the case, with the iNKT cell subset showing on average ~1.7-fold brighter CD11a staining than tetramer-negative T cells (Figure 1A, right plot).

We next investigated the impact of ICAM-1 exposure on iNKT cell IFN-γ secretion in response to IL-12. Human iNKT cells were incubated in culture medium containing recombinant human IL-12p70 in the presence or absence of plate-bound ICAM-1-Fc for 24h. Culture supernatants were harvested and tested for secreted IFN-γ by ELISA. While exposure to IL-12 alone was sufficient to induce iNKT cell IFN-γ secretion, the IFN-γ amounts were consistently elevated in the presence of plate-bound ICAM-1-Fc (Figure 1B), suggesting that ICAM-1 exposure co-stimulated the IL-12-driven IFN-γ production. Since LFA-1 is comprised of two subunits, CD11a (integrin α L) and CD18 (integrin β 2), we tested the involvement of each of the subunits. iNKT cells were incubated with IL-12 and plate-bound ICAM-1-Fc in the presence or absence of blocking antibodies against CD11a and CD18. Blockade of either CD11a or CD18 resulted in abrogation of the ICAM-dependent enhancement of iNKT cell IFN-γ secretion, and anti-CD11a blockade completely abrogated the response (Figure 1C). Together, these results demonstrate that ICAM-1 binding to LFA-1 co-stimulates iNKT cell IFN-γ secretion that is driven by IL-12.

LFA-1 stimulation alone is sufficient to induce iNKT cell IFN-γ secretion

To further investigate the requirements for ICAM-1 to promote IFN-γ secretion by iNKT cells, we titrated the density of the plate-bound ICAM-1-Fc. Low densities of ICAM-1-Fc showed no detectable co-stimulatory effect, but as the density increased we observed an abrupt enhancement of iNKT cell IFN-γ secretion in response to IL-12 (Figure 2A, grey circle symbols). Surprisingly, however, at densities of ICAM-1-Fc above this inflection point we observed that iNKT cell IFN-γ secretion was induced even in the absence of IL-12 (Figure 2A, black triangle symbols). Addition of even high doses of an inhibitor of JAK, which is required for IL-12-mediated activation of iNKT cells, did not abolish the iNKT cell IFN-γ secretion induced by exposure to high density ICAM-1-Fc, whereas it did abrogate the iNKT cell response to IL-12 cytokine (Figure 2B). These observations suggested that

ICAM-1 exposure drives IFN-γ secretion by iNKT cells directly via signaling through LFA-1, in a manner that does not require signaling through a JAK2-dependent pathway

To confirm that CD1d recognition is not required for iNKT cell activation by ICAM-Fc, we tested the effect of inclusion of an anti-CD1d blocking antibody. Whereas the presence of an anti-CD1d mAb significantly reduced iNKT cell IFN-γ secretion in response to plate-bound CD1d-Fc pulsed with the α-Gal-Cer lipid antigen, there was no detectable impact on iNKT cell activation by plate-bound ICAM-Fc (Figure 2C). We also noted that most of the cultured iNKT cells used for these experiments showed no detectable cell surface expression of CD1d (Supplementary Figure 2A), and we have not observed α-GalCer lipid antigen-mediated activation of cultured iNKT cells in the absence of $CD1d^+$ APCs (Supplementary Figure 2B). Thus, exposure to high-density ICAM-1 appears to activate iNKT cells independently of CD1d recognition.

While signaling through the IL-12 receptor does not induce Ca^{++} flux in T cells, LFA-1 ligation can induce re-organization of the actin cytoskeleton in T cells that leads to both Ca^{++} signaling and c-Jun N-terminal kinase (JNK) activation (33, 35). Therefore, we assessed cytoplasmic calcium levels in iNKT cells exposed to an ICAM-1 coated surface. iNKT cells were cytoplasmically labeled with Fluo-4, a dye that increases its fluorescence in proportion to the surrounding Ca^{++} concentration, and placed onto glass slides coated with ICAM-1-Fc and blocked with poly-L-Lysine. Microscopic imaging revealed that iNKT cells placed on slides coated either with poly-L-lysine alone or with a negative control immunoglobulin showed little evidence of Ca^{++} signaling (Figure 3A and B). Exposure to slides coated with 1 μg/ml ICAM-1-Fc resulted in only a minimal increase in Fluo-4 signal, but iNKT cells placed on slides coated with 5 μg/ml ICAM-1-Fc showed significantly elevated Fluo-4 signal (Figure 3A and B). Moreover, analysis of the Fluo-4 signal intensity over time for a selection of individual iNKT cells revealed greater spiking of Fluo-4 signal intensity over time in the high-density ICAM-1 exposed iNKT cells compared to those in the poly-L-Lysine control condition (Figure 3C). To assess the importance of Ca^{++} signaling for IFN-γ production by iNKT cells in response to high-density ICAM-1, we tested the effect of cyclosporine A (CsA), a drug that not only inhibits the Ca^{++}-dependent serine phosphatase calcineurin, but that also blocks the activation of JNK and p38 MAPK signaling pathways (60). iNKT cells were exposed to plate-bound ICAM-1-Fc or anti-CD3 mAb as a positive control, in the presence of titrated concentrations of CsA. IFN-γ secretion in response to either anti-CD3 or ICAM-1 was completely abrogated in the presence of CsA (Figure 3D). Together, these results suggest that LFA-1 engagement by a high density of ICAM-1 induces signaling in iNKT cells that leads to IFN-γ production.

We previously observed that contact with APCs potentiates iNKT cell secretion of IFN-γ in response to subsequent IL-12 exposure, and this effect is highly dependent on activation of ERK in the iNKT cells (46). To investigate whether MAPK signaling may play a role in LFA-1 mediated activation of iNKT cells, we first confirmed that anti-CD11a mAb stimulation is sufficient to induce ERK phosphorylation in Jurkat T cells. Jurkat cells were exposed to anti-CD11a mAb stimulation for varying amounts of time, then Western blotting of lysates was performed to detect total or phosphorylated ERK. As shown in Figure 4A, anti-CD11a mAb treatment resulted in ERK phosphorylation, with signals peaking after 6–9

minutes of stimulation, and then declining. We also observed phosphorylated ERK after stimulation of primary PBMCs directly *ex vivo*, and the p-ERK signal was selectively inhibited in the presence of U0126 (Figure 4B). Stimulation of cultured human iNKT cells with an anti-CD11a mAb reproducibly resulted in ERK phosphorylation as detected by Western blotting, and this was abrogated by U0126 treatment (Figure 4C). Moreover, intracellular flow cytometric analysis confirmed that CD11a-stimulated iNKT cells showed specific staining for p-ERK (Figure 4D). To evaluate whether ERK phosphorylation was required for iNKT cell IFN-γ secretion in response to ICAM-1, iNKT cells were incubated on ICAM-1-Fc coated plates or with anti-CD3 mAb, in the presence of titrated concentrations of U0126. While the iNKT cell IFN-γ response to anti-CD3 mAb stimulation was partially inhibited by U0126, the response to plate-bound ICAM-1-Fc was almost completely abrogated by the presence of U0126 (Figure 4E). Thus, compared to TCR-activation, iNKT cell IFN-γ secretion in response to LFA-1 stimulation appears to be more highly dependent on ERK signaling.

ICAM-1 exposure induces IFN-γ production by human innate lymphocytes directly ex vivo

We next investigated whether exposure to an ICAM-coated surface was sufficient to induce IFN-γ production by primary cells. Freshly isolated human PBMCs were incubated for 14–24 hours (the final 12 hours in the presence of monensin) in culture wells coated with 5 μg/ml ICAM-1-Fc or with an isotype-matched negative control mAb. The cells were resuspended, stained for cell surface markers, then fixed and permeabilized and stained to assess intracellular IFN-γ. Flow cytometric analysis revealed that a small fraction (typically 0.5–1%) of the lymphocyte population produced IFN-γ after exposure to plate-bound ICAM-1-Fc, but not to the isotype-matched control mAb (Figure 5A). The cells that produced IFN-γ after ICAM-exposure had higher expression of CD11a (LFA-1) compared to those that did not respond (Figure 5B), although, notably, not all of the $CD11a^{hi}$ cells showed IFN-γ production (Figure 5A). Similar to what we had observed for cultured iNKT cells, this response was abrogated by the presence of either CsA or U0126 (Figure 5C and D).

We used t-Distributed Stochastic Neighbor Embedding (tSNE) dimensionality reduction of a series of multi-parameter flow cytometric analyses to assess the peripheral blood lymphocyte populations containing the responding cells. Since we had observed that the cells that produced IFN-γ in response to plate-bound ICAM-1-Fc had elevated CD11a expression, we mapped the levels of CD11a staining of cell types within the peripheral blood lymphocyte gate. Whereas B cells showed CD11a staining that was on the low end of the spectrum, and most CD4 T cells expressed moderate CD11a levels, high levels of CD11a were predominant on NK cells, CD8αα and on a fraction of CD8β T cells and double-negative (DN) T cells (Figure 6A, left plots). Analysis of the specific innate lymphocyte populations (NK cells, iNKT cells, MAIT cells, $V\delta2^+$ T cells) within PBMC samples of a group of unrelated healthy adults revealed that each of these subsets had significantly elevated CD11a expression compared to the total T cell population (Figure 6A, right plot). Thus, for our further analyses we gated on $CD11a^{hi}$ lymphocytes.

Analysis of CD11a^{hi} lymphocytes from PBMC samples stimulated by exposure to plate-bound ICAM-1-Fc revealed that IFN-γ producing cells were distributed within the NK cell and T cell populations, with a trend towards co-localization with populations that co-expressed CD56 and CD161, and partial overlap with cells that expressed PLZF (Figure 6B, left plots). Typically, the majority of the responding cells were T cells, while the remainder were NK cells (Figure 6B, right plot). Using TCR-specific reagents we observed that IFN-γ-producing cells were found within the iNKT cell, MAIT cell, and Vδ2^{+} T cell subsets (Figure 6C). These results suggest that the ability to produce IFN-γ directly in response to a high surface density of ICAM-1 is a shared feature of human innate T lymphocytes and NK cells.

Discussion

The results presented here delineate a novel pathway of integrin-mediated T cell activation. While prior studies have emphasized the ability of LFA-1 to contribute to T cell activation by lowering the threshold required for productive TCR signaling (34, 35), we show here that innate T lymphocytes can directly utilize LFA-1 signaling to activate IFN-γ secretion. Since LFA-1 ligation occurs in the context of interactions with ICAM^{+} APCs, and LFA-1 engagement can enhance IFN-γ secretion in response to IL-12 stimulation, this activation pathway may facilitate the targeting of IFN-γ secretion towards specific types of recipient cells during inflammatory responses. Moreover, since IL-12 is not required, LFA-1-mediated activation may allow innate T cells to promulgate inflammatory responses independently of myeloid APCs in situations where an initiating event has led to the up-regulation of ICAM on other cell types. For example, events such as the deposition of oxidized LDL or exposure to TNFα or IL-1β are known to upregulate expression of ICAM-1 on vascular endothelial cells (61, 62). Since IFN-γ induces the upregulation of adhesion molecules on vascular endothelial cells, the integrin-mediated activation of iNKT cells in this context might play a role at the earliest stages of plaque formation by promoting the initial arrest of monocytic cells. Thus, we hypothesize that integrin-mediated activation of iNKT cells not only contributes to their responses during interactions with APCs that express CD1d and/or produce IL-12, but may also allow them to carry out functions in previously unrecognized situations where such APCs are not necessarily present.

One of the key features of the LFA-1-mediated activation pathway we observed is that it requires a threshold density of ICAM-1 in order to activate iNKT cell IFN-γ secretion. This may not be surprising, since it is known that LFA-1 binding to ICAM-1 involves a complex interplay between the conformational state of the LFA-1 molecule, (which can adopt low, intermediate, or high affinity states), and the avidity status induced by activation-induced clustering of LFA-1 at the cell surface (30). Thus, it is possible that the presence of a comparatively high density of ICAM-1 is sufficient to induce conformational changes in the LFA-1 molecules expressed by innate T lymphocytes that are associated with de novo signal transduction. It is intriguing to speculate that the high cell surface expression level of LFA-1 on innate T cells is thus a critical aspect of their ability to undergo independent LFA-mediated activation, since their elevated level of LFA-1 may enhance avidity-based interactions with ICAM.

We show here that activation of iNKT cells by LFA-1 involves both Ca^{++} and ERK signaling. We have previously demonstrated that human iNKT cells are highly responsive to weak TCR stimulation that generates ERK phosphorylation but only a minimal level of Ca^{++} signaling (47). Moreover, we found that weak TCR engagement (even when it is not sufficient to directly induce a productive response) leads to acetylation of the IFNG locus of iNKT cells, and this epigenetic status renders them receptive to TCR-independent stimulation by IL-12 and IL-18 (46). It thus seems likely that the epigenetic status of the IFNG locus of innate T lymphocytes may also play a critical role in their ability to produce IFN-γ in response to LFA-1-mediated signals. Notably, while our studies suggest that CD1d recognition is not required for the activation of iNKT cells by high-density ICAM-1, since CD1d is present on a variety of cell types, and the TCRs of human iNKT cells can bind with low-affinity to broadly distributed self-lipids (e.g. lyso-phosphatidylcholine), it is not clear whether ICAM-1-mediated activation is likely to occur physiologically in the absence of TCR-stimulation.

However, our prior studies have suggested that human iNKT cells that are activated by weak TCR-agonists (e.g. CD1d-presenting self antigens) produce mainly GM-CSF, and not IFN-γ (47). In contrast, we noted that iNKT cell activation by high-density ICAM-1-Fc appears to selectively induced IFN-γ secretion, with little evidence of other cytokines typically produced by human iNKT cells, such as GM-CSF, IL-13, or IL-4 (data not shown). Thus, the presence of elevated ICAM-1 expression levels may serve to bias iNKT cell responses towards a Th1-phenotype even in the absence of strong TCR agonists or IL-12. Consistent with this, a prior report has also suggested that LFA-1 engagement promotes Th1 functions in iNKT cells (63).

This analysis outlines a previously unrecognized pathway of innate T cell activation that relies on signals resulting from LFA-1 binding to ICAM-1. It will be of significant interest in the future to determine whether this pathway allows innate T cells to influence other cell types in previously unrecognized situations. For example, naive T cells undergoing TCR-mediated activation have been shown to up-regulate their cell surface ICAM-1 and form clusters with other T cells (64). LFA-1 induced IFN-γ secreted by iNKT cells in this context could thus promote Th1-polarization of naive T lymphocytes. Such interactions might contribute to the remarkable ability of iNKT cells to promote antigen-specific responses by adaptive T lymphocytes (65–70).

Supplementary Material

Refer to Web version on PubMed Central for supplementary material.

Acknowledgments

Financial Support

Funding provided by NIH R01AI074940 and R21AI116007 to JEG.

References

1. Alonzo ES, and Sant'Angelo DB 2011 Development of PLZF-expressing innate T cells. Curr Opin Immunol 23: 220–227. [PubMed: 21257299]
2. Constantinides MG, McDonald BD, Verhoef PA, and Bendelac A 2014 A committed precursor to innate lymphoid cells. Nature 508: 397–401. [PubMed: 24509713]
3. Eidson M, Wahlstrom J, Beaulieu AM, Zaidi B, Carsons SE, Crow PK, Yuan J, Wolchok JD, Horsthemke B, Wieczorek D, and Sant'Angelo DB 2011 Altered development of NKT cells, gammadelta T cells, CD8 T cells and NK cells in a PLZF deficient patient. PLoS One 6: e24441. [PubMed: 21915328]
4. Constantinides MG, and Bendelac A 2013 Transcriptional regulation of the NKT cell lineage. Cur. Opin. Immunol 25: 161–167.
5. Kovalovsky D, Uche OU, Eladad S, Hobbs RM, Yi W, Alonzo E, Chua K, Eidson M, Kim HJ, Im JS, Pandolfi PP, and Sant'Angelo DB 2008 The BTB-zinc finger transcriptional regulator PLZF controls the development of invariant natural killer T cell effector functions. Nat Immunol 9: 1055–1064. [PubMed: 18660811]
6. Savage AK, Constantinides MG, Han J, Picard D, Martin E, Li B, Lantz O, and Bendelac A 2008 The transcription factor PLZF directs the effector program of the NKT cell lineage. Immunity 29: 391–403. [PubMed: 18703361]
7. Lantz O, and Bendelac A 1994 An invariant T cell receptor alpha chain is used by a unique subset of major histocompatibility complex class I-specific CD4+ and CD4–8- T cells in mice and humans. J. Exp. Med 180: 1097–1106. [PubMed: 7520467]
8. Bendelac A, Lantz O, Quimby ME, Yewdell JW, Bennink JR, and Brutkiewicz RR 1995 CD1 recognition by mouse NK1+ T lymphocytes. Science 268: 863–865. [PubMed: 7538697]
9. Kawano T, Cui J, Koezuka Y, Toura I, Kaneko Y, Motoki K, Ueno H, Nakagawa R, Sato H, Kondo E, Koseki H, and Taniguchi M 1997 CD1d-restricted and TCR-mediated activation of valpha14 NKT cells by glycosylceramides. Science 278: 1626–1629. [PubMed: 9374463]
10. Brossay L, Chioda M, Burdin N, Koezuka Y, Casorati G, Dellabona P, and Kronenberg M 1998 CD1d-mediated recognition of an alpha-galactosylceramide by natural killer T cells is highly conserved through mammalian evolution. J. Exp. Med 188: 1521–1528. [PubMed: 9782129]
11. Cui Y, Franciszkiewicz K, Mburu YK, Mondot S, Le Bourhis L, Premel V, Martin E, Kachaner A, Duban L, Ingersoll MA, Rabot S, Jaubert J, De Villartay JP, Soudais C, and Lantz O 2015 Mucosal-associated invariant T cell-rich congenic mouse strain allows functional evaluation. J Clin Invest 125: 4171–4185. [PubMed: 26524590]
12. Alonzo ES, Gottschalk RA, Das J, Egawa T, Hobbs RM, Pandolfi PP, Pereira P, Nichols KE, Koretzky GA, Jordan MS, and Sant'Angelo DB 2010 Development of promyelocytic zinc finger and ThPOK-expressing innate gamma delta T cells is controlled by strength of TCR signaling and Id3. J Immunol 184: 1268–1279. [PubMed: 20038637]
13. Treiner E, Duban L, Bahram S, Radosavljevic M, Wanner V, Tilloy F, Affaticati P, Gilfillan S, and Lantz O 2003 Selection of evolutionarily conserved mucosal-associated invariant T cells by MR1. Nature 422: 164–169. [PubMed: 12634786]
14. Le Bourhis L, Guerri L, Dusseaux M, Martin E, Soudais C, and Lantz O 2011 Mucosal-associated invariant T cells: unconventional development and function. Trends Immunol 32: 212–218. [PubMed: 21459674]
15. Kjer-Nielsen L, Patel O, Corbett AJ, Le Nours J, Meehan B, Liu L, Bhati M, Chen Z, Kostenko L, Reantragoon R, Williamson NA, Purcell AW, Dudek NL, McConville MJ, O'Hair RA, Khairallah GN, Godfrey DI, Fairlie DP, Rossjohn J, and McCluskey J 2012 MR1 presents microbial vitamin B metabolites to MAIT cells. Nature 491: 717–723. [PubMed: 23051753]
16. Beetz S, Wesch D, Marischen L, Welte S, Oberg HH, and Kabelitz D 2008 Innate immune functions of human gammadelta T cells. Immunobiology 213: 173–182. [PubMed: 18406365]
17. Adams EJ, Gu S, and Luoma AM 2015 Human gamma delta T cells: Evolution and ligand recognition. Cell Immunol 296: 31–40. [PubMed: 25991474]
18. Gu S, Borowska MT, Boughter CT, and Adams EJ 2018 Butyrophilin3A proteins and Vgamma9Vdelta2 T cell activation. Semin Cell Dev Biol.

19. Bendelac A, Bonneville M, and Kearney JF 2001 Autoreactivity by design: innate B and T lymphocytes. Nat Rev Immunol 1: 177–186. [PubMed: 11905826]
20. Cohen NR, Brennan PJ, Shay T, Watts GF, Brigl M, Kang J, and Brenner MB 2013 Shared and distinct transcriptional programs underlie the hybrid nature of iNKT cells. Nat Immunol 14: 90–99. [PubMed: 23202270]
21. Thomas SY, Scanlon ST, Griewank KG, Constantinides MG, Savage AK, Barr KA, Meng F, Luster AD, and Bendelac A 2011 PLZF induces an intravascular surveillance program mediated by long-lived LFA-1-ICAM-1 interactions. J Exp Med 208: 1179–1188. [PubMed: 21624939]
22. Smith A, Stanley P, Jones K, Svensson L, McDowall A, and Hogg N 2007 The role of the integrin LFA-1 in T-lymphocyte migration. Immunol Rev 218: 135–146. [PubMed: 17624950]
23. Emoto M, Mittrucker HW, Schmits R, Mak TW, and Kaufmann SH 1999 Critical role of leukocyte function-associated antigen-1 in liver accumulation of CD4+NKT cells. J Immunol 162: 5094–5098. [PubMed: 10227978]
24. Thanabalasuriar A, Neupane AS, Wang J, Krummel MF, and Kubes P 2016 iNKT Cell Emigration out of the Lung Vasculature Requires Neutrophils and Monocyte-Derived Dendritic Cells in Inflammation. Cell Rep 16: 3260–3272. [PubMed: 27653688]
25. Aslanian AM, Chapman HA, and Charo IF 2005 Transient role for CD1d-restricted natural killer T cells in the formation of atherosclerotic lesions. Arterioscler Thromb Vasc Biol 25: 628–632. [PubMed: 15591216]
26. Bobryshev YV, and Lord RS 2005 Co-accumulation of dendritic cells and natural killer T cells within rupture-prone regions in human atherosclerotic plaques. J Histochem Cytochem 53: 781–785. [PubMed: 15928327]
27. Chan WL, Pejnovic N, Hamilton H, Liew TV, Popadic D, Poggi A, and Khan SM 2005 Atherosclerotic abdominal aortic aneurysm and the interaction between autologous human plaque-derived vascular smooth muscle cells, type 1 NKT, and helper T cells. Circ Res 96: 675–683. [PubMed: 15731463]
28. Nakai Y, Iwabuchi K, Fujii S, Ishimori N, Dashtsoodol N, Watano K, Mishima T, Iwabuchi C, Tanaka S, Bezbradica JS, Nakayama T, Taniguchi M, Miyake S, Yamamura T, Kitabatake A, Joyce S, Van Kaer L, and Onoe K 2004 Natural killer T cells accelerate atherogenesis in mice. Blood 104: 2051–2059. [PubMed: 15113755]
29. Kyriakakis E, Cavallari M, Andert J, Philippova M, Koella C, Bochkov V, Erne P, Wilson SB, Mori L, Biedermann BC, Resink TJ, and De Libero G 2010 Invariant natural killer T cells: Linking inflammation and neovascularization in human atherosclerosis. Eur J Immunol.
30. Springer TA, and Dustin ML 2012 Integrin inside-out signaling and the immunological synapse. Curr Opin Cell Biol 24: 107–115. [PubMed: 22129583]
31. Kanner SB, Grosmaire LS, Ledbetter JA, and Damle NK 1993 Beta 2-integrin LFA-1 signaling through phospholipase C-gamma 1 activation. Proc Natl Acad Sci U S A 90: 7099–7103. [PubMed: 7688472]
32. Evans R, Lellouch AC, Svensson L, McDowall A, and Hogg N 2011 The integrin LFA-1 signals through ZAP-70 to regulate expression of high-affinity LFA-1 on T lymphocytes. Blood 117: 3331–3342. [PubMed: 21200022]
33. Sirim P, Zeitlmann L, Kellersch B, Falk CS, Schendel DJ, and Kolanus W 2001 Calcium signaling through the beta 2-cytoplasmic domain of LFA-1 requires intracellular elements of the T cell receptor complex. J Biol Chem 276: 42945–42956. [PubMed: 11559699]
34. Perez OD, Mitchell D, Jager GC, South S, Murriel C, McBride J, Herzenberg LA, Kinoshita S, and Nolan GP 2003 Leukocyte functional antigen 1 lowers T cell activation thresholds and signaling through cytohesin-1 and Jun-activating binding protein 1. Nat Immunol 4: 1083–1092. [PubMed: 14528303]
35. Suzuki J, Yamasaki S, Wu J, Koretzky GA, and Saito T 2007 The actin cloud induced by LFA-1-mediated outside-in signals lowers the threshold for T-cell activation. Blood 109: 168–175. [PubMed: 16973965]
36. Sidobre S, Naidenko OV, Sim BC, Gascoigne NR, Garcia KC, and Kronenberg M 2002 The V alpha 14 NKT cell TCR exhibits high-affinity binding to a glycolipid/CD1d complex. J Immunol 169: 1340–1348. [PubMed: 12133957]

37. Crowe NY, Uldrich AP, Kyparissoudis K, Hammond KJ, Hayakawa Y, Sidobre S, Keating R, Kronenberg M, Smyth MJ, and Godfrey DI 2003 Glycolipid antigen drives rapid expansion and sustained cytokine production by NK T cells. J Immunol 171: 4020–4027. [PubMed: 14530322]
38. Kain L, Webb B, Anderson BL, Deng S, Holt M, Costanzo A, Zhao M, Self K, Teyton A, Everett C, Kronenberg M, Zajonc DM, Bendelac A, Savage PB, and Teyton L 2014 The identification of the endogenous ligands of natural killer T cells reveals the presence of mammalian alpha-linked glycosylceramides. Immunity 41: 543–554. [PubMed: 25367571]
39. Kain L, Costanzo A, Webb B, Holt M, Bendelac A, Savage PB, and Teyton L 2015 Endogenous ligands of natural killer T cells are alpha-linked glycosylceramides. Molec. Immunol 68: 94–97. [PubMed: 26141240]
40. Fox LM, Cox DG, Lockridge JL, Wang X, Chen X, Scharf L, Trott DL, Ndonye RM, Veerapen N, Besra GS, Howell AR, Cook ME, Adams EJ, Hildebrand WH, and Gumperz JE 2009 Recognition of lyso-phospholipids by human natural killer T lymphocytes. PLoS Biol 7: e1000228. [PubMed: 19859526]
41. Lopez-Sagaseta J, Sibener LV, Kung JE, Gumperz J, and Adams EJ 2012 Lysophospholipid presentation by CD1d and recognition by a human Natural Killer T-cell receptor. Embo J 31: 2047–2059. [PubMed: 22395072]
42. Ortaldo JR, Young HA, Winkler-Pickett RT, Bere EW, Jr., Murphy WJ, and Wiltrout RH 2004 Dissociation of NKT stimulation, cytokine induction, and NK activation in vivo by the use of distinct TCR-binding ceramides. J Immunol 172: 943–953. [PubMed: 14707067]
43. Pellicci DG, Clarke AJ, Patel O, Mallevaey T, Beddoe T, Le Nours J, Uldrich AP, McCluskey J, Besra GS, Porcelli SA, Gapin L, Godfrey DI, and Rossjohn J 2011 Recognition of beta-linked self glycolipids mediated by natural killer T cell antigen receptors. Nat Immunol 12: 827–833. [PubMed: 21804559]
44. Nagarajan NA, and Kronenberg M 2007 Invariant NKT cells amplify the innate immune response to lipopolysaccharide. J Immunol 178: 2706–2713. [PubMed: 17312112]
45. Tyznik AJ, Tupin E, Nagarajan NA, Her MJ, Benedict CA, and Kronenberg M 2008 Cutting edge: the mechanism of invariant NKT cell responses to viral danger signals. J Immunol 181: 4452–4456. [PubMed: 18802047]
46. Wang X, Bishop KA, Hegde S, Rodenkirch LA, Pike JW, and Gumperz JE 2012 Human invariant natural killer T cells acquire transient innate responsiveness via histone H4 acetylation induced by weak TCR stimulation. J Exp Med 209: 987–1000. [PubMed: 22508835]
47. Wang X, Chen X, Rodenkirch L, Simonson W, Wernimont S, Ndonye RM, Veerapen N, Gibson D, Howell AR, Besra GS, Painter GF, Huttenlocher A, and Gumperz JE 2008 Natural killer T-cell autoreactivity leads to a specialized activation state. Blood 112: 4128–4138. [PubMed: 18779390]
48. Holzapfel KL, Tyznik AJ, Kronenberg M, and Hogquist KA 2014 Antigen-dependent versus -independent activation of invariant NKT cells during infection. J Immunol 192: 5490–5498. [PubMed: 24813205]
49. Brigl M, Bry L, Kent SC, Gumperz JE, and Brenner MB 2003 Mechanism of CD1d-restricted natural killer T cell activation during microbial infection. Nat Immunol 4: 1230–1237. [PubMed: 14578883]
50. Mattner J, Debord KL, Ismail N, Goff RD, Cantu C, 3rd, Zhou D, Saint-Mezard P, Wang V, Gao Y, Yin N, Hoebe K, Schneewind O, Walker D, Beutler B, Teyton L, Savage PB, and Bendelac A 2005 Exogenous and endogenous glycolipid antigens activate NKT cells during microbial infections. Nature 434: 525–529. [PubMed: 15791258]
51. Brigl M, Tatituri RV, Watts GF, Bhowruth V, Leadbetter EA, Barton N, Cohen NR, Hsu FF, Besra GS, and Brenner MB 2011 Innate and cytokine-driven signals, rather than microbial antigens, dominate in natural killer T cell activation during microbial infection. J Exp Med 208: 1163–1177. [PubMed: 21555485]
52. Huse M, Lillemeier BF, Kuhns MS, Chen DS, and Davis MM 2006 T cells use two directionally distinct pathways for cytokine secretion. Nat Immunol 7: 247–255. [PubMed: 16444260]
53. Volkov Y, Long A, and Kelleher D 1998 Inside the crawling T cell: leukocyte function-associated antigen-1 cross-linking is associated with microtubule-directed translocation of protein kinase C isoenzymes beta(I) and delta. J Immunol 161: 6487–6495. [PubMed: 9862672]

54. Velazquez P, Cameron TO, Kinjo Y, Nagarajan N, Kronenberg M, and Dustin ML 2008 Cutting edge: activation by innate cytokines or microbial antigens can cause arrest of natural killer T cell patrolling of liver sinusoids. J Immunol 180: 2024–2028. [PubMed: 18250405]

55. Brigl M, van den Elzen P, Chen X, Meyers JH, Wu D, Wong CH, Reddington F, Illarianov PA, Besra GS, Brenner MB, and Gumperz JE 2006 Conserved and heterogeneous lipid antigen specificities of CD1d-restricted NKT cell receptors. J Immunol 176: 3625–3634. [PubMed: 16517731]

56. Chen X, Wang X, Besra GS, and Gumperz JE 2007 Modulation of CD1d-restricted NKT cell responses by CD4. J Leukoc Biol 82: 1455–1465. [PubMed: 17726154]

57. Chen X, Wang X, Keaton JM, Reddington F, Illarionov PA, Besra GS, and Gumperz JE 2007 Distinct endosomal trafficking requirements for presentation of autoantigens and exogenous lipids by human CD1d molecules. J Immunol 178: 6181–6190. [PubMed: 17475845]

58. Hegde S, Chen X, Keaton JM, Reddington F, Besra GS, and Gumperz JE 2007 NKT cells direct monocytes into a DC differentiation pathway. J Leukoc Biol 81: 1224–1235. [PubMed: 17311932]

59. Xu X, Pocock GM, Sharma A, Peery SL, Fites JS, Felley L, Zarnowski R, Stewart D, Berthier E, Klein BS, Sherer NM, and Gumperz JE 2016 Human iNKT Cells Promote Protective Inflammation by Inducing Oscillating Purinergic Signaling in Monocyte-Derived DCs. Cell Rep 16: 3273–3285. [PubMed: 27653689]

60. Matsuda S, and Koyasu S 2000 Mechanisms of action of cyclosporine. Immunopharmacology 47: 119–125. [PubMed: 10878286]

61. Amberger A, Maczek C, Jurgens G, Michaelis D, Schett G, Trieb K, Eberl T, Jindal S, Xu Q, and Wick G 1997 Co-expression of ICAM-1, VCAM-1, ELAM-1 and Hsp60 in human arterial and venous endothelial cells in response to cytokines and oxidized low-density lipoproteins. Cell Stress Chaperones 2: 94–103. [PubMed: 9250400]

62. Takei A, Huang Y, and Lopes-Virella MF 2001 Expression of adhesion molecules by human endothelial cells exposed to oxidized low density lipoprotein. Influences of degree of oxidation and location of oxidized LDL. Atherosclerosis 154: 79–86. [PubMed: 11137085]

63. Matsumoto G, Kubota E, Omi Y, Lee U, and Penninger JM 2004 Essential role of LFA-1 in activating Th2-like responses by alpha-galactosylceramide-activated NKT cells. J Immunol 173: 4976–4984. [PubMed: 15470040]

64. Zumwalde NA, Domae E, Mescher MF, and Shimizu Y 2013 ICAM-1-dependent homotypic aggregates regulate CD8 T cell effector function and differentiation during T cell activation. J Immunol 191: 3681–3693. [PubMed: 23997225]

65. Iwamura C, Shinoda K, Endo Y, Watanabe Y, Tumes DJ, Motohashi S, Kawahara K, Kinjo Y, and Nakayama T 2012 Regulation of memory CD4 T-cell pool size and function by natural killer T cells in vivo. Proc Natl Acad Sci U S A 109: 16992–16997. [PubMed: 23027937]

66. Chang DH, Osman K, Connolly J, Kukreja A, Krasovsky J, Pack M, Hutchinson A, Geller M, Liu N, Annable R, Shay J, Kirchhoff K, Nishi N, Ando Y, Hayashi K, Hassoun H, Steinman RM, and Dhodapkar MV 2005 Sustained expansion of NKT cells and antigen-specific T cells after injection of alpha-galactosyl-ceramide loaded mature dendritic cells in cancer patients. J Exp Med 201: 1503–1517. [PubMed: 15867097]

67. Silk JD, Hermans IF, Gileadi U, Chong TW, Shepherd D, Salio M, Mathew B, Schmidt RR, Lunt SJ, Williams KJ, Stratford IJ, Harris AL, and Cerundolo V 2004 Utilizing the adjuvant properties of CD1d-dependent NK T cells in T cell-mediated immunotherapy. J Clin Invest 114: 1800–1811. [PubMed: 15599405]

68. Li K, Luo J, Wang C, and He H 2011 alpha-Galactosylceramide potently augments M2e-induced protective immunity against highly pathogenic H5N1 avian influenza virus infection in mice. Vaccine 29: 7711–7717. [PubMed: 21839133]

69. Johnson TR, Hong S, Van Kaer L, Koezuka Y, and Graham BS 2002 NK T cells contribute to expansion of CD8(+) T cells and amplification of antiviral immune responses to respiratory syncytial virus. J. Virol 76: 4294–4303. [PubMed: 11932395]

70. Guillonneau C, Mintern JD, Hubert FX, Hurt AC, Besra GS, Porcelli S, Barr IG, Doherty PC, Godfrey DI, and Turner SJ 2009 Combined NKT cell activation and influenza virus vaccination

boosts memory CTL generation and protective immunity. Proc Natl Acad Sci U S A 106: 3330–3335. [PubMed: 19211791]

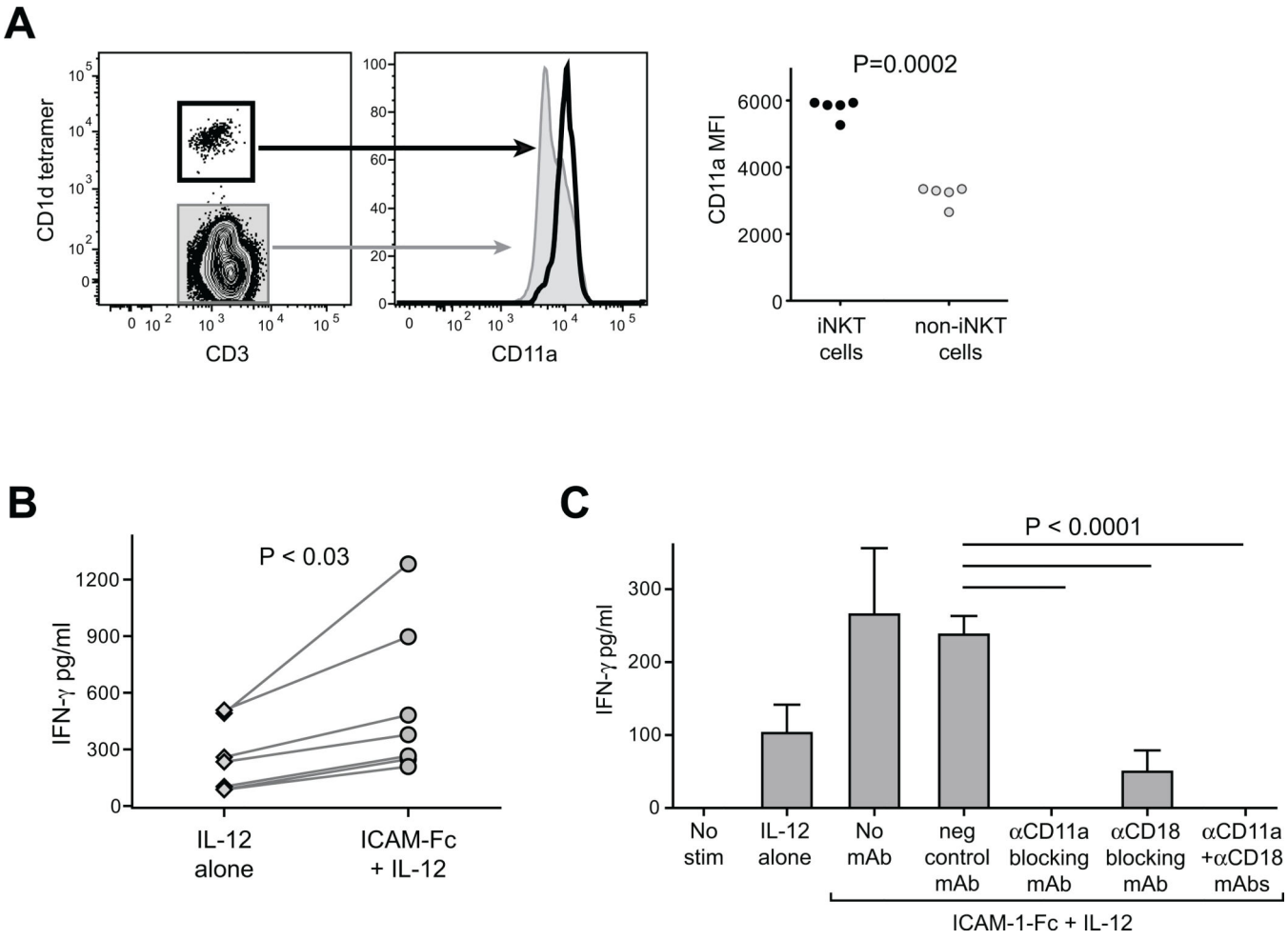

Figure 1. Elevated LFA-1 expression on human iNKT cells co-stimulates IFN-γ secretion in response to IL-12p70.

A) Freshly isolated human PBMCs were stained with antibodies against CD3 and CD11a, and with α-GalCer loaded CD1d tetramer and analyzed by flow cytometry. Plots on left show CD11a expression by CD1d-tetramer positive (heavy black line) compared to tetramer-negative (grey shaded) for one representative experiment. Plot on right shows results from analysis of PBMC samples from five unrelated healthy adults. Mean fluorescence intensity (MFI) of CD11a staining is plotted for CD1d-tetramer positive (iNKT cells) and tetramer-negative (non-iNKT cells). **B)** iNKT cells were incubated for 24h in medium containing 20 U/ml recombinant human IL-12p70, in the presence of plate-bound ICAM-1-Fc (coated at 5 μg/ml) or negative control mAb ("IL-12 alone"). Secreted IFN-γ was quantitated using a standardized ELISA. The plot shows aggregated results from 7 independent experiments, using 5 different iNKT cell clonal lines (clones PP1.2, PP1.3, PP1.10, J3N.5, GG1.2). **C)** iNKT cells were incubated for 24h in culture medium alone ("no stim"), or in medium containing IL-12p70 in wells coated with a negative control mAb ("IL-12 alone"), or in medium containing IL-12p70 in wells coated with ICAM-1-Fc in the presence or absence of the indicated blocking antibodies, and secreted IFN-γ was quantitated by ELISA. The plot shows results from one representative experiment out of two using a short-term *in vitro*

expansion of poly-clonal iNKT cells (318D line); bars indicate means and standard deviations from 4 replicates per treatment. Similar results were observed in an additional independent experiments (once with the 318D line, and once with iNKT clone PP1.2).

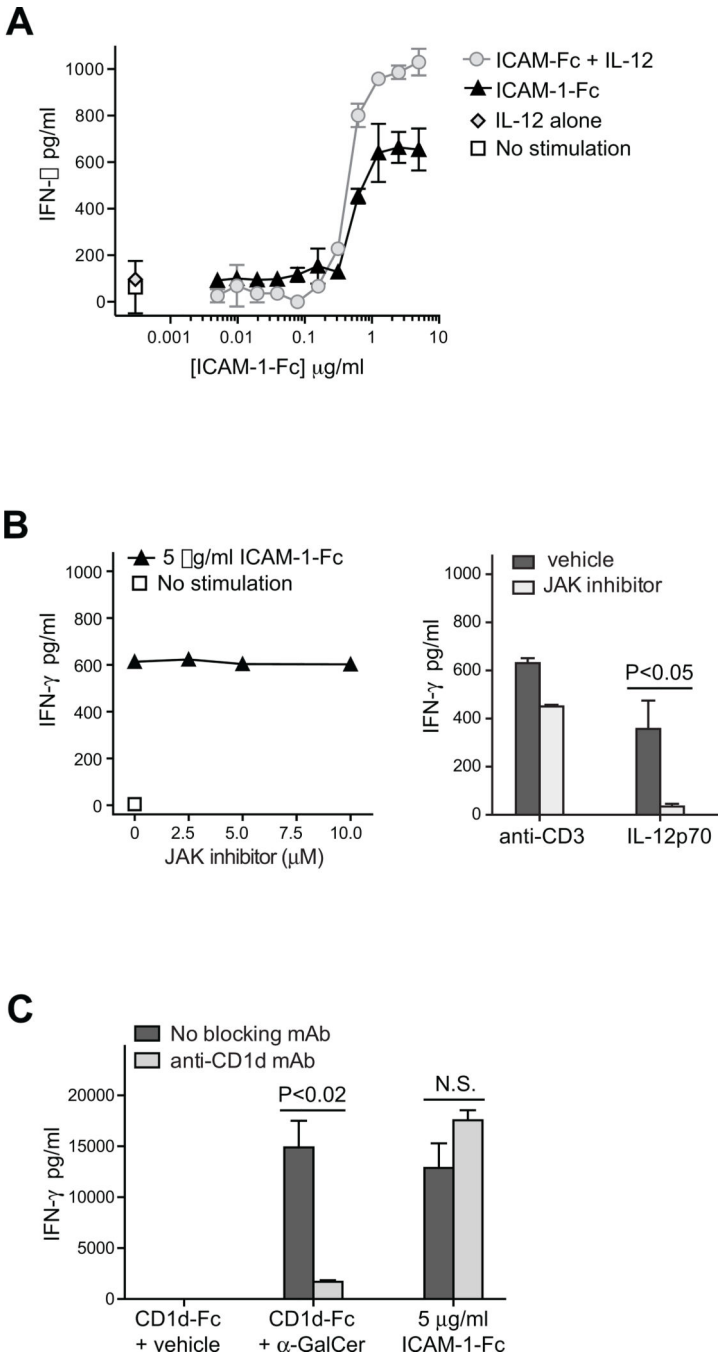

Figure 2. Exposure to a high density of ICAM-1 promotes iNKT cell IFN-γ secretion in a manner that is independent of IL-12 stimulation and CD1d recognition.

A) iNKT cells were incubated for 24h in wells coated with the indicated titrated doses of ICAM-1-Fc, in the presence or absence of 20 U/ml IL-12p70. Secreted IFN-γ was quantitated by ELISA. The plot shows results from one representative experiment out of two using a short-term *in vitro* expansion of poly-clonal iNKT cells (FoB line); symbols indicate means and standard deviations four replicates per treatment. Similar results were observed in an additional independent experiment using iNKT clones PP1.2. **B)** Left plot: iNKT cells

(318D short-term polyclonal line) were incubated in wells coated with ICAM-1-Fc in the presence of the indicated concentrations of JAK2 inhibitor and secreted IFN-γ was quantitated by ELISA; similar results were obtained using a different polyclonal iNKT line (4LF). Right plot: iNKT cells (318D short-term polyclonal line) were exposed to plate-bound anti-CD3 mAb or cultured in medium containing IL-12p70, in the presence or absence of 10 μM JAK2 inhibitor. **C)** iNKT cells (318D short-term polyclonal line) were incubated in wells coated with CD1d-Fc fusion protein that had been pulsed with 25 ng/ml α-GalCer or vehicle, or in wells coated with 5 μg/ml ICAM-1-Fc. Where indicated, the CD1d- or ICAM-mediated iNKT cell stimulation was performed in the presence of an anti-CD1d blocking mAb.

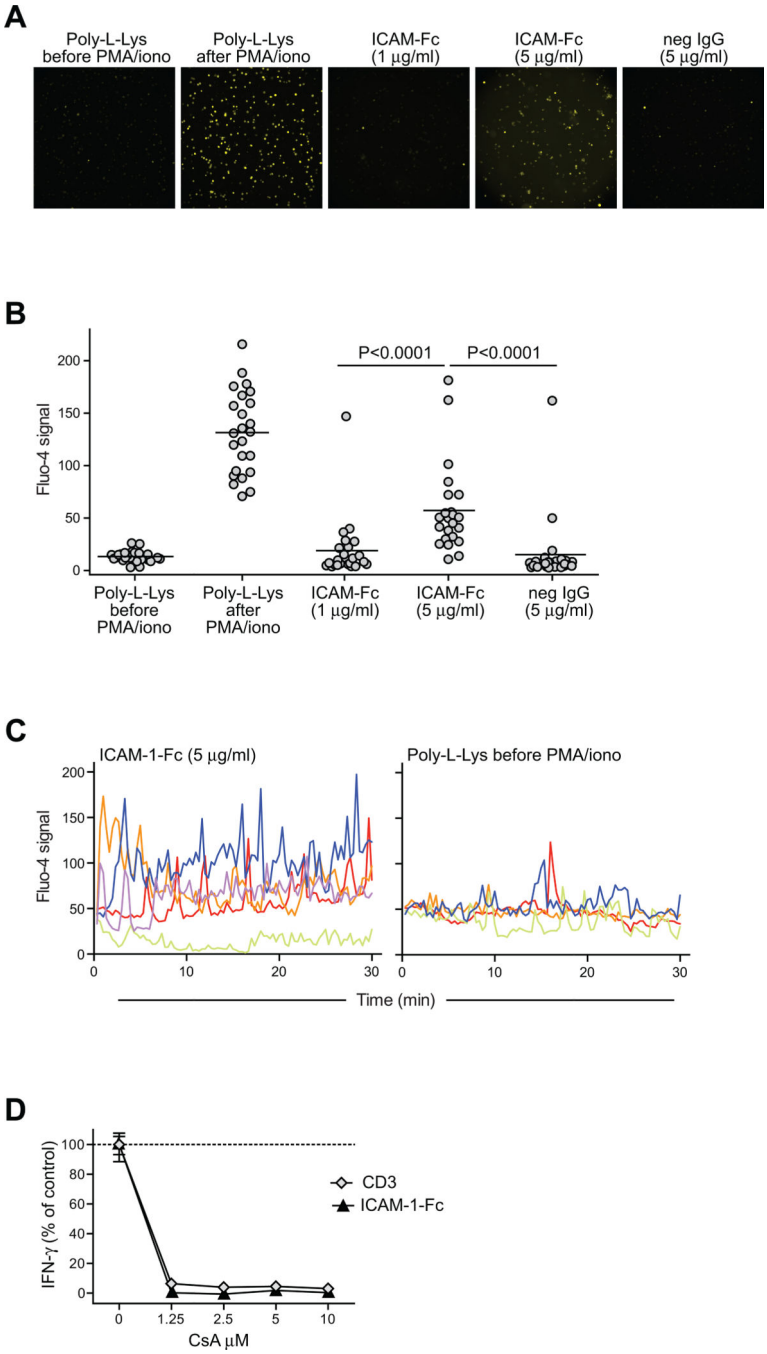

Figure 3. Exposure to high density ICAM-1 induces Ca^{++} signaling in iNKT cells.

A-C) Cultured human iNKT cells (318D short-term polyclonal line) labeled with the calcium indicator dye Fluo-4 were placed on slides coated with the concentrations of ICAM-1-Fc, or with 5 µg/ml negative control immunoglobulin, or with poly-L-Lysine alone. Images were taken at 20 second intervals using a fluorescence microscope. Panel (**A**) shows a fluorescence microscopic image for each of the conditions. Panel (**B**) shows results from quantitation of the fluorescence signal for 24 randomly chosen cells per condition. Panel (**C**) shows the Fluo-4 signal intensities over time for individual iNKT cells (indicated by

different color lines) placed on slides coated with 5 μg/ml ICAM or poly-L-lysine alone. **D)** iNKT cells were incubated for 24h with plate-bound ICAM-1-Fc (coated at 5 μg/ml), or with 0.5 μg/ml soluble anti-CD3 mAb, in the presence of the indicated concentrations of cyclosporin A (CsA), and secreted IFN-γ was quantitated by ELISA. The plot shows the amount of IFN-γ as a percentage of the amount produced in each condition in the absence of CsA; symbols represent the means and standard deviations (not always visible on the scale shown) of four replicates per condition. Similar results were obtained in four independent analyses.

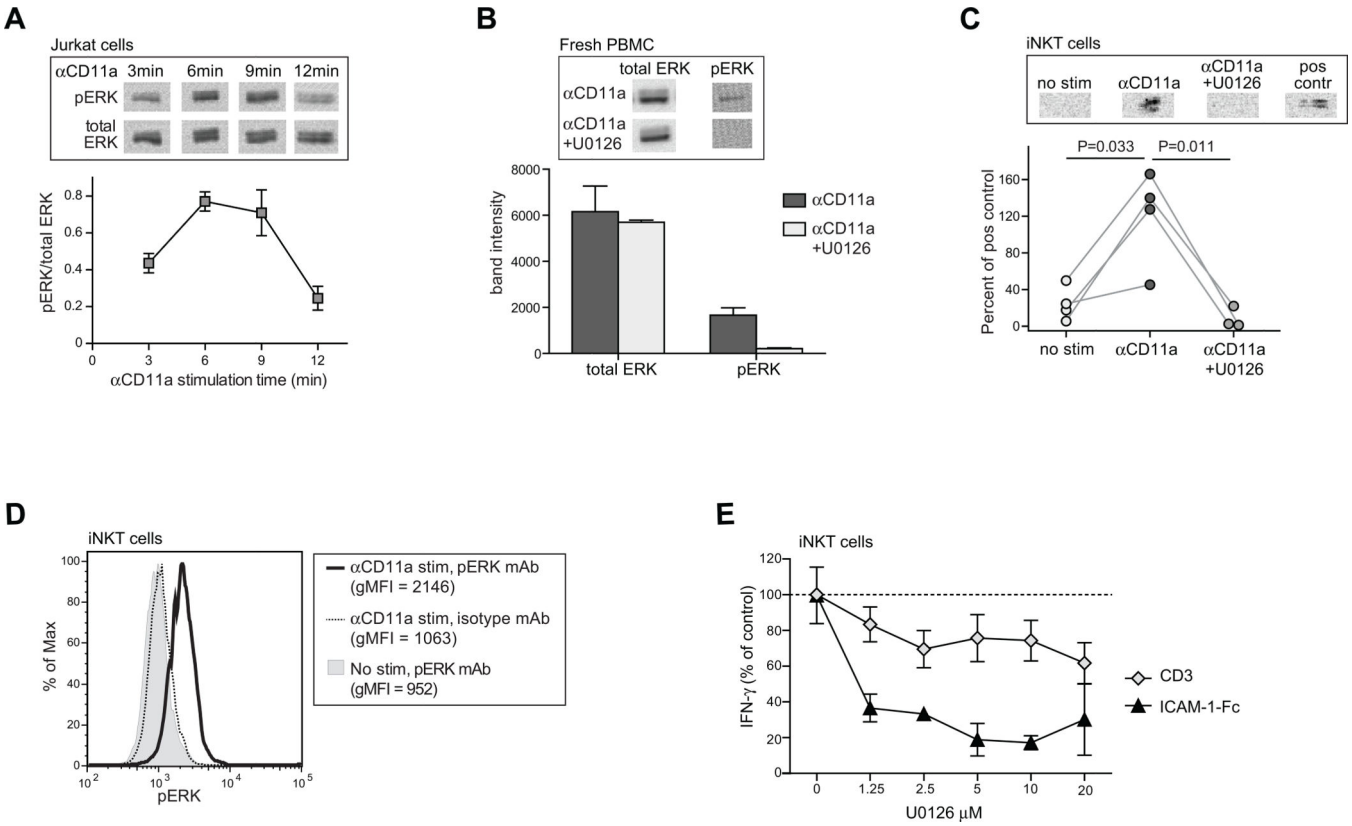

Figure 4. iNKT cell IFN-γ secretion in response to LFA-1 stimulation is dependent on ERK phosphorylation.

A) Jurkat T cells were stimulated with anti-CD11a mAb for the indicated times, then lysed and subjected to Western blotting using detection antibodies against either total ERK or phospho-ERK. Images at the top show the phospho-ERK and corresponding total ERK results from a representative Western blot analysis; the plot below shows the means and standard deviations of the phospho-ERK signal normalized by the corresponding total ERK signal from three replicate Western blot analyses. **B)** Freshly isolated PBMCs were stimulated for 5 min with anti-CD11a in the presence or absence of 5 μM of the MEK inhibitor U0126. Images at the top show phospho-ERK and corresponding total ERK Western blot results. The plot below shows the band intensity (mean, std dev)from 3 independent analyses. **C**) Cultured iNKT cells (FoB short-term polyclonal line) were stimulated with anti-CD11a mAb for 5 minutes in the presence or absence of 5 μM U0126 and lysates were Western blotted to detect phospho-ERK. Positive control indicates Jurkat cells that were stimulated with 20nM 12-O-Tetradecanoyl-phorbol-13-acetate for 10 minutes. Plot below shows the aggregated results from 4 independent analyses, with band intensities for iNKT cell p-ERK normalized by the signal from the corresponding positive control band run in parallel. **D**) iNKT cells (318D short-term polyclonal line) were stimulated with anti-CD11a mAb for 5 minutes or mock-treated, then fixed and permeabilized, stained using an antibody against p-ERK or an isotype-matched negative control, and analyzed by flow cytometry. **E)** iNKT cells (FoB short-term polyclonal line) were incubated for 24h with plate-bound ICAM-1-Fc or with soluble anti-CD3 mAb, in the presence of the indicated concentrations of U0126, and secreted IFN-γ was quantitated by

ELISA. The plot shows the amount of IFN-γ as a percentage of the amount produced in each condition in the absence of U0126; symbols represent the means and standard deviations (not always visible on the scale shown) of four replicates. Similar results were obtained in two additional independent analyses using the FoB polyclonal and PP1.3 clonal iNKT cell lines.

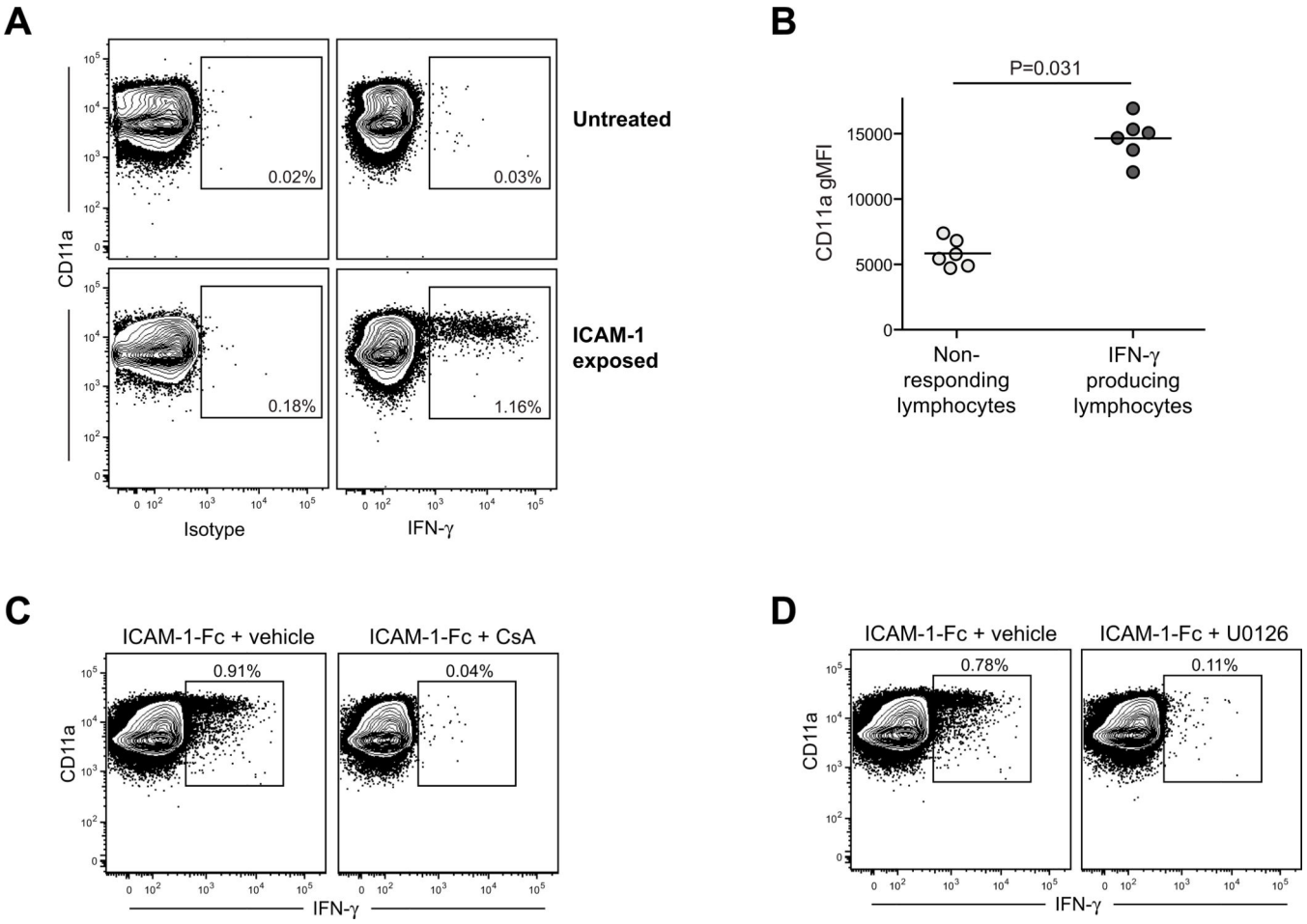

Figure 5. Exposure to high density ICAM-1 activates IFN-γ production by a small subset of human lymphocytes directly *ex vivo*.

A) Freshly isolated human PBMCs were incubated in culture wells coated with 5 μg/ml ICAM-1-Fc or with an isotype-matched negative control mAb, then subjected to flow cytometric analysis to assess CD11a expression levels and intracellular IFN-γ. Plots show results from analysis of the total lymphocyte gate as assessed by forward and side scatter. **B)** Aggregated results from analyses of PBMCs from six unrelated healthy adults, showing CD11a geometric mean fluorescence intensity (gMFI) for the lymphocyte population that stained positively for IFN-γ compared to those that did not. **C and D)** Freshly isolated human PBMCs were incubated in culture wells coated with 5 μg/ml ICAM-1-Fc in the presence of 5μM CsA (panel **C**) or 5μM U0126 (panel **D**), or vehicle alone, and then subjected to flow cytometric analysis to assess CD11a expression levels and intracellular IFN-γ.

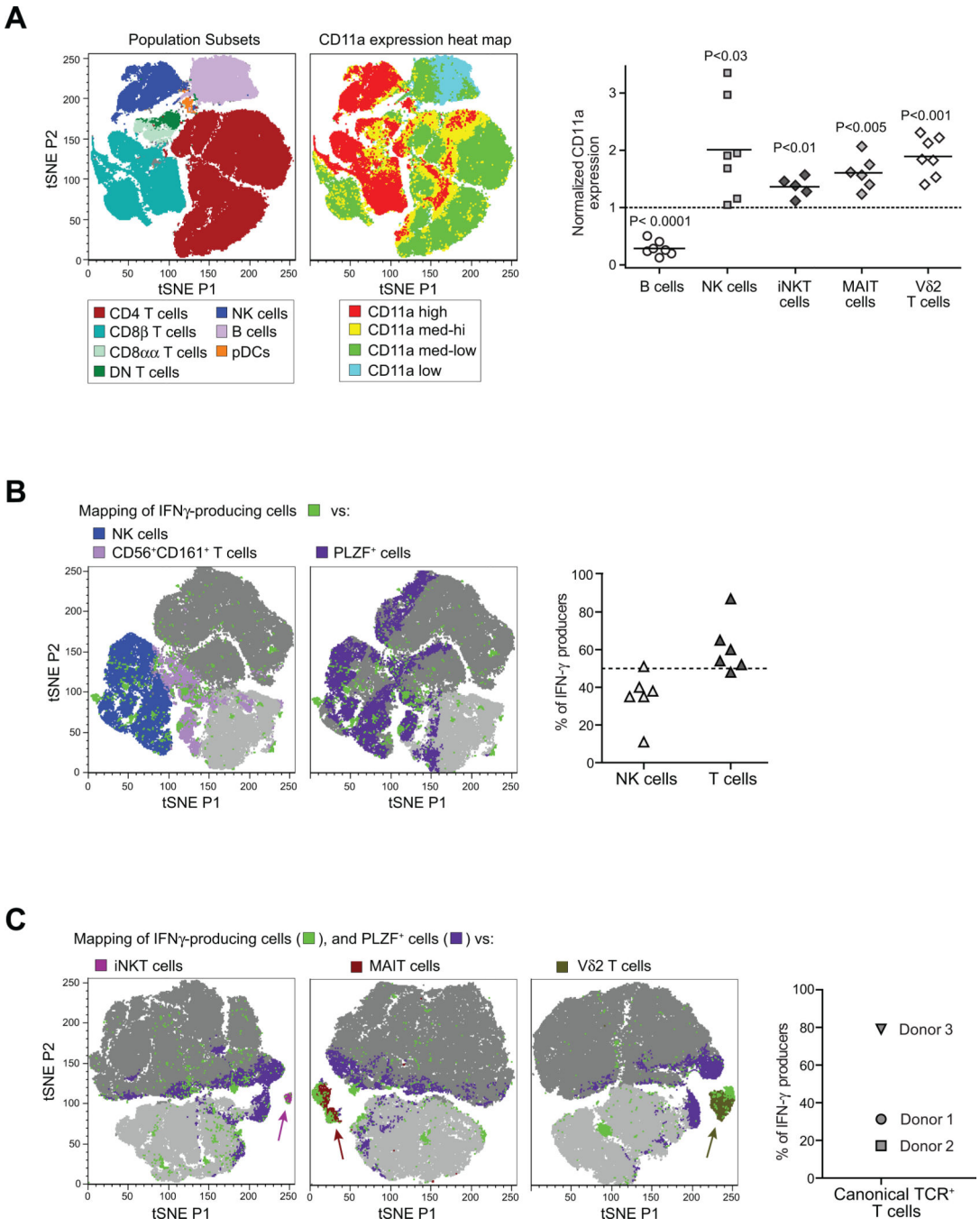

Figure 6. NK cells and innate T cells produce IFN-γ directly *ex vivo* in response to high density ICAM-1.

Freshly isolated human PBMCs were incubated in wells coated with 5 μg/ml ICAM-1-Fc, then analyzed by flow cytometry to characterize the IFN-γ producing cells. A) Left plots: A freshly isolated PBMC sample was stained with antibodies against CD3, CD4, CD8α, CD8β, CD56, and CD11a, and analyzed by t-Distributed Stochastic Neighbor Embedding (tSNE) dimensionality reduction. Plot on left shows how lymphocyte subsets within the sample were clustered by the tSNE analysis. Neighboring plot shows the relative expression levels of CD11a for the cells included in the same tSNE analysis. Graph on far right shows

the aggregated results from analysis of CD11a expression levels on the indicated lymphocyte subsets from PBMC samples of unrelated healthy adult donors. Each symbol represents the gMFI of the CD11a staining for the indicated cell type normalized by the CD11a gMFI of the total T cell population from the sam PBMC sample. B) Freshly isolated PBMC samples were exposed *ex vivo* to plate-bound ICAM-1-Fc, then stained with antibodies against CD3, CD8β, CD56, CD161, CD11a, and fixed and permeabilized and stained for intracellular IFN-γ and PLZF. Flow cytometric staining results from three independent PBMC samples were concatenated, and the $CD11a^{hi}$ lymphocytes were subjected to tSNE analysis. Far left plot shows the distribution of NK cells, $CD56^{+}CD161^{+}$ T cells and IFN-γ^{+} cells (light grey in background corresponds to $CD8\beta^{+}$ T cells; dark grey corresponds to all other cells). Neighboring plot shows the distribution of $PLZF^{+}$ and IFN-γ^{+} cells. Scatter plot on right shows the fraction of the IFN-γ producing subset identified as NK cells ($CD56^{+}CD3^{-}$) vs. T cells ($CD3^{+}CD56^{-}$) for PBMC samples from six unrelated healthy adults. C) Freshly isolated PBMC samples exposed to plate-bound ICAM-1, were stained for CD3, CD8β, CD161, CD11a, IFN-γ, PLZF, and either CD1d-tetramer, MR1-tetramer, or Vδ2 TCR. Results from three independent identically stained PBMC samples were concatenated, and the $CD11a^{hi}$ T cells were subjected to tSNE analysis. tSNE plots show the presence of IFN-γ^{+} cells in the iNKT (far left), MAIT (middle), and $V\delta2^{+}$ T cell (right) subsets. Graph on far right shows the percent of the IFN-γ-producing population expressing these canonical TCRs for each of the PBMC donors that were included in the tSNE analyses.